JOURNAL OF GUIDANCE, CONTROL, AND DYNAMICS
Vol. 17, No. 6, November–December 1994

Derivation of System Matrices from Nonlinear Dynamic Simulation of Jet Engines

N. Sugiyama*
National Aerospace Laboratory, Chofu, Tokyo 182, Japan

Most multivariable control design methodologies are linear theories and utilize a linearized plant model. Since accuracy of a linearized plant model affects the quality of a control system designed by those methods, a reasonable linearized plant model that adequately simulates the plant must be prepared. This paper describes a derivation method of such a model in the form of *ABCD* system matrices from nonlinear dynamic simulation. System matrices of a two-spool turbofan engine are derived and compared to the actual engine data. The effect of perturbation size and linearization formula over a linearized model are discussed. A corrected form of the system matrices is introduced to extend the data base to the whole flight envelope.

Nomenclature

$A, B, \hat{B}, C, D, \hat{D}, P, Q$	= matrix
$a_{ij}, b_{il}, \hat{b}_{il}, c_{kj}, d_{kl}, \hat{d}_{kl}, p_{jl}, q_{kl}$	= element of matrix
$f(\cdot), g(\cdot), h(\cdot)$	= function of $(\cdot)$
G	= transfer function
I	= identity matrix
u, x, y	= vector
u, x, y	= element of u, x, y
δ	= absolute perturbation size
ϵ	= relative perturbation size or convergent index
λ	= eigenvalue

Engine Variables

F	= engine thrust
h	= enthalpy
I	= moment of inertia
M	= flight Mach number
m	= stored mass in volume
N, N_h, N_l	= rotational speed
P	= total pressure
Q	= excess power of rotor
T	= total temperature or torque
V	= intercomponent volume
W	= gas flow rate
W_f	= fuel flow rate
u	= stored energy in volume
α	= stator angle
δ	= total pressure at engine inlet divided by standard pressure
θ	= total temperature at engine inlet divided by standard temperature

Subscripts

h, l	= high- and low-pressure rotor
in, out	= inlet and outlet of volume
2, 21, 3, 4, 41, ...	= engine station number

Presented as Paper 92-3319 at the AIAA/SAE/ASME/ASEE 28th Joint Propulsion Conference, Nashville, TN, July 6–8, 1992; received July 31, 1992; revision received Dec. 17, 1993; accepted for publication April 5, 1994.

*Head, Engine Control Laboratory, Aero Engine Division. Member AIAA.

I. Introduction

FOR higher performance and multimission requirements, modern gas turbine engines are becoming more and more complex in engine cycles and geometries. Such an engine is an inherently nonlinear multivariable system and has numerous variable geometry features, such as variable nozzle, variable stator, etc., to realize the optimum performance. Hence the requirements for engine control systems are becoming more and more severe due to the complexity of the static and dynamic behavior of an engine and increasing number of control variables. Multivariable control concepts such as linear quadratic regulator (LQR) theory, H_∞ theory, μ-synthesis, etc., must be applied to efficiently design such control systems.

Most multivariable control design methodologies are linear theories and utilize a linearized plant model. The accuracy of a linearized plant model affects the quality of the control system designed by those methods and is important to the practical application of modern multivariable control theories.

A linearized plant model is obtained by 1) linearization of nonlinear dynamic simulation[1–3] or 2) some identification techniques.[4] The former method can generate a reasonable linearized plant model simply and efficiently. The feature of the latter method is that the same identification software can be applied to both an actual plant and a simulated plant. Some existing simulation softwares[5,6] include these capabilities, but the user must utilize those with great care because a linearized model is very sensitive to the method applied. This paper describes a derivation method of a linearized plant model in the form of *ABCD* system matrices from nonlinear dynamic simulation. As an example, system matrices of a two-spool turbofan engine are derived and compared with the actual engine data. The effect of perturbation size and a linearization formula over a linearized model is discussed. Then the corrected form of system matrices is introduced to extend the data base to the whole flight envelope.

II. Linearization

A nonlinear time-invariant system is expressed as follows:
State equation:

$$\dot{x} = f(x, u) \tag{1}$$

Output equation:

$$y = g(x, u) \tag{2}$$

where $x \in R^n$, $y \in R^m$, and $u \in R^r$. Expanding Eqs. (1) and (2) about an arbitrary operating point (x_a, u_a), using the multivariable Taylor theorem, and neglecting second-order small yield the following:
State equation:

$$\delta\dot{x} = A\delta x + B\delta u \tag{3}$$

Output equation:

$$\delta y = C\delta x + D\delta u \tag{4}$$

where $\delta x = x - x_a$, $\delta \dot{x} = \dot{x} - \dot{x}_a$, $\delta y = y - y_a$, $\delta u = u - u_a$, $y_a = g(x_a, u_a)$, and $\dot{x}_a = f(x_a, u_a)$. The system matrices A, B, C, and D are $n \times n$, $n \times r$, $m \times n$, and $m \times r$, respectively, and are defined as follows:

State matrix:

$$A = [a_{ij}] = \left[\frac{\partial f_i}{\partial x_j}\right] \tag{5}$$

Control matrix:

$$B = [b_{il}] = \left[\frac{\partial f_i}{\partial u_l}\right] \tag{6}$$

Output matrix:

$$C = [c_{kj}] = \left[\frac{\partial g_k}{\partial x_j}\right] \tag{7}$$

Direct couple matrix:

$$D = [d_{kl}] = \left[\frac{\partial g_k}{\partial u_l}\right] \tag{8}$$

where $i = 1, 2, \ldots, n$, $j = 1, 2, \ldots, n$, $k = 1, 2, \ldots, m$, and $l = 1, 2, \ldots, r$. The term $\partial f_i / \partial x_j$ represents the partial derivative of $f_i(x_1, x_2, \ldots, u_1, u_2, \ldots)$ with respect to x_j, evaluated at an arbitrary point, $(x_{a1}, x_{a2}, \ldots, u_{a1}, u_{a2}, \ldots)$, and so on.

If x and u are changed in keeping the steady-state relations,

$$f(x, u) = 0 \qquad \text{or} \qquad x = h(u) \tag{9}$$

Matrices B and D are defined differently using matrices A and C in Eqs. (5) and (7) as follows:

$$\hat{B} = [\hat{b}_{il}] = -\left[\sum_{j=1}^{n} a_{ij}\left(\frac{\partial x_j}{\partial u_l}\right)_{f=0}\right] = -AP \tag{10}$$

$$\hat{D} = [\hat{d}_{kl}] = \left[\left(\frac{\partial g_k}{\partial u_l}\right)_{f=0} - \sum_{j=1}^{n} c_{kj}\left(\frac{\partial x_j}{\partial u_l}\right)_{f=0}\right] = Q - CP \tag{11}$$

$$P = [p_{jl}] = \left[\left(\frac{\partial x_j}{\partial u_l}\right)_{f=0}\right] \tag{12}$$

$$Q = [q_{kl}] = \left[\left(\frac{\partial g_k}{\partial u_l}\right)_{f=0}\right] = \left[\left(\frac{\partial y_k}{\partial u_l}\right)_{f=0}\right] \tag{13}$$

where $i = 1, 2, \ldots, n$, $k = 1, 2, \ldots, m$, and $l = 1, 2, \ldots, r$. Matrices P and Q are $n \times r$ and $m \times r$, respectively. The term $(\partial x_j / \partial u_l)_{f=0}$ is the partial derivative of $h_j(u_1, u_2, \ldots)$ with respect to u_l, evaluated at the steady-state point $(u_{s1}, u_{s2}, \ldots)$. This method is called the forced match method.[3] If x_j is measurable, $(\partial x_j / \partial u_l)_{f=0}$ in Eq. (12) can be obtained from steady-state data of the actual plant. The discrepancy between the actual plant and simulation is inevitable, and hence the linearized model using actual plant data results in better steady-state relations.

III. Computation of Partials

Partial derivatives a_{ij}, b_{il}, c_{kj}, and d_{kl} in Eqs. (5–8) are computed by perturbing state variables x and control variables u. Two perturbation methods are considered. One is relative perturbation and takes the form $x(1+\epsilon)$. The other is absolute perturbation and takes the form $x + \delta$. When the absolute value of x is unknown, the former generates proper perturbation. But when $x = 0$, the latter must be used since the former cannot generate perturbation. Letting the perturbation size $x\epsilon = \delta$, both methods are equivalent. Also computation of partial derivative a_{ij} is similar to that of the rest, b_{il}, c_{kj}, d_{kl}.

Hence the computational formula for a_{ij} in absolute perturbation is derived below:

Two-point Lagrange formula (forward or backward):

$$a_{ij} = \frac{f_i(x_j + \delta_{xj}) - f_i(x_j)}{\delta_{xj}} \qquad \text{or} \qquad \frac{f_i(x_j) - f_i(x_j - \delta_{xj})}{\delta_{xj}} \tag{14}$$

Three-point Lagrange formula:

$$a_{ij} = \frac{f_i(x_j + \delta_{xj}) - f_i(x_j - \delta_{xj})}{2\delta_{xj}} \tag{15}$$

Five-point Lagrange formula:

$$a_{ij} = \frac{-f_i(x_j+2\delta_{xj}) + 8f_i(x_j+\delta_{xj}) - 8f_i(x_j - \delta_{xj}) + f_i(x_j - 2\delta_{xj})}{12\delta_{xj}} \tag{16}$$

Five-point cubic spline formula (equally spaced, natural spline):

$$a_{ij} = \frac{-f_i(x_j+2\delta_{xj}) + 6f_i(x_j+\delta_{xj}) - 6f_i(x_j-\delta_{xj}) + f_i(x_j - 2\delta_{xj})}{8\delta_{xj}} \tag{17}$$

where $i = 1, 2, \ldots, n$, $j = 1, 2, \ldots, n$. The term δ_{xj} is the perturbation size for the jth state variable x_j; $f_i(x_j + \delta_{xj})$ is the ith function value at the point $x_1, \ldots, x_j + \delta_{xj}, \ldots, x_n, u_1, \ldots, u_r$. Two- and four-point function evaluation is sufficient for a three- and five-point symmetric formula as above.

Partial derivatives $\hat{b}_{il}$, $\hat{d}_{kl}$, p_{jl}, q_{kl} in Eqs. (10–13) are computed by perturbing control variables u and keeping the steady-state condition (9). The computational formulas for p_{jl}, q_{kl} are similar to Eqs. (14–17). For example, the three-point formula is as follows:

$$p_{jl} = \frac{h_j(u_l + \delta_{ul}) - h_j(u_l - \delta_{ul})}{2\delta_{ul}} \tag{18}$$

where $j = 1, 2, \ldots, n$, $l = 1, 2, \ldots, r$. Here, δ_{ul} is the perturbation size for the lth control variable u_l; $h_j(u_l \pm \delta_{ul})$ is the steady-state value of the jth state variable x_j for the control value of $(u_1, u_2, \ldots, u_l \pm \delta_{ul}, \ldots, u_r)$.

The steady-state value of state x, corresponding to the specified value of control u, is computed efficiently by a Newton-Raphson procedure using the A matrix obtained in Eq. (5). A Newton-Raphson iteration formula from the N step to the $N+1$ step,

$$x_{N+1} = x_N - \left(\frac{\partial f}{\partial x}\right)_N^{-1} \cdot f(x_N, u) = x_N - A_N^{-1} \cdot f(x_N, u) \tag{19}$$

is repeated until the convergent condition $|x_{N+1} - x_N| \leq \epsilon$ is satisfied. Equation (19) is rearranged as follows:

$$A_N \cdot (x_{N+1} - x_N) = -f(x_N, u) \tag{20}$$

This is a simultaneous linear algebraic equation with a coefficient matrix A_N and is solved for $x_{N+1} - x_N$ by existing software. Here, x_{N+1} is obtained more efficiently by Eq. (20) than by Eq. (19) because the computational time of a matrix inverse is approximately three times as long as that of simultaneous linear algebraic equations.

The above procedure can be included in a nonlinear simulation software. In general, a dynamic simulation software repeats the following steps: 1) evaluates the right-hand side (RHS) of the simultaneous nonlinear differential equations (1); 2) integrates Eq. (1) numerically using the RHS of previous steps, $f(x_N, u_N), f(x_{N-1}, u_{N-1}), \ldots$; and 3) sets state variables for the next step, x_{N+1}. The computations of Eqs. (14–18) are similar to this process, i.e., 1) set state variables perturbed one at a time, 2) evaluate the RHS, and 3) compute system matrices. Hence this procedure can be included only by modification of the numerical integration routine. The computations of Eq. (19), which is almost the same in form as the Euler integration formula, can be also included.

IV. Nonlinear Dynamic Simulation of Jet Engines

To illustrate the method developed here, a nonlinear dynamic simulation of a two-spool turbofan engine is considered. The above-mentioned procedure is mechanized on an ultra-high-speed digital simulator, designated the AD100[7] system, and combined with the simulation software developed by the author,[8] which can simulate various types of gas turbine engines at real-time or faster-than-real-time speeds with high fidelity and flexibility.

Figure 1 shows the schematic configuration of a two-spool turbofan engine. Engine component performance data and some overall performance data, including dynamic performance, for this engine are available. Control variables are fuel flow rate W_f and the variable stator angle of a high-pressure compressor, α.

The schematic model in Fig. 1 can be diagrammed as shown in Fig. 2, replacing the engine components with the computational modules developed in Ref. 8. In this simulation, computational modules for compressor (COMP), turbine (TURB), nozzle (NOZL), combustor (COMB), duct (DUCT), bleed (BLEED), inlet (INLET), rotor (ROTOR), and volume (VOL) are used. Among these modules, the rotor and volume are dynamic modules and the rest are static modules.

The mathematical model of static modules is based on thermo- and aerodynamic relations and performance maps. The mathematical model of rotor dynamics is based on the conservation of angular momentum:

$$\dot{N} = \frac{Q}{IN} = \frac{T}{I} \tag{21}$$

where N is the rotational speed of the rotor in radians per second, I is the polar moment of inertia, T is torque, and Q is excess power or acceleration power, defined as a difference between turbine power and compressor power, $Q = Q_t - Q_c$. The mathematical model of volume dynamics is based on the conservation of mass and energy:

$$\dot{m} = \sum W_{\text{in}} - \sum W_{\text{out}} \tag{22}$$

$$\dot{u} = \sum W_{\text{in}} h_{\text{in}} - \sum W_{\text{out}} h_{\text{out}} \tag{23}$$

Therefore, one state variable exists in a rotor module and two state variables in a volume module.

Figure 2 shows that the whole simulation model of this engine includes 2 rotors and 7 volumes, resulting in 16 state variables totally. Hence state vector $\boldsymbol{x}$ is defined as

$$\boldsymbol{x} = (N_h, N_l, m_{21}, u_{21}, m_3, u_3, m_4, u_4, m_{41}, u_{41}, m_5, u_5, m_{3B}, u_{3B}, m_{5B}, u_{5B})' \tag{24}$$

where N_h is the high-pressure rotor speed, N_l the low-pressure rotor speed, m_{21} the stored mass at volume 21, u_{21} the stored energy at volume 21, and so on. The prime notation denotes a matrix transpose.

Control vector $\boldsymbol{u}$ is defined as

$$\boldsymbol{u} = (W_f, \alpha)' \tag{25}$$

where, W_f is the fuel flow rate and α the stator angle of the compressor.

Output vector $\boldsymbol{y}$, which can be defined as arbitrary, should include representative variables of engine or measurable variables:

$$\boldsymbol{y} = (N_h, N_l, P_3, F)' \tag{26}$$

where P_3 is the compressor outlet pressure and F the thrust.

The linear model of a two-spool turbofan engine includes 16 state variables, 2 control variables, and 4 output variables. Sensor and actuator dynamics are not considered in this paper.

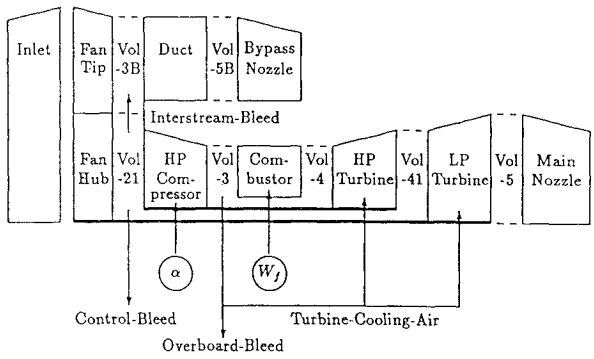

Fig. 1 Configuration of two-spool turbofan engine.

V. System Matrices of Jet Engine

A. Effect of Perturbation Size and Formula

Since a ruling factor in the transient behavior of an engine is rotor dynamics, system matrix elements or partial derivatives pertaining

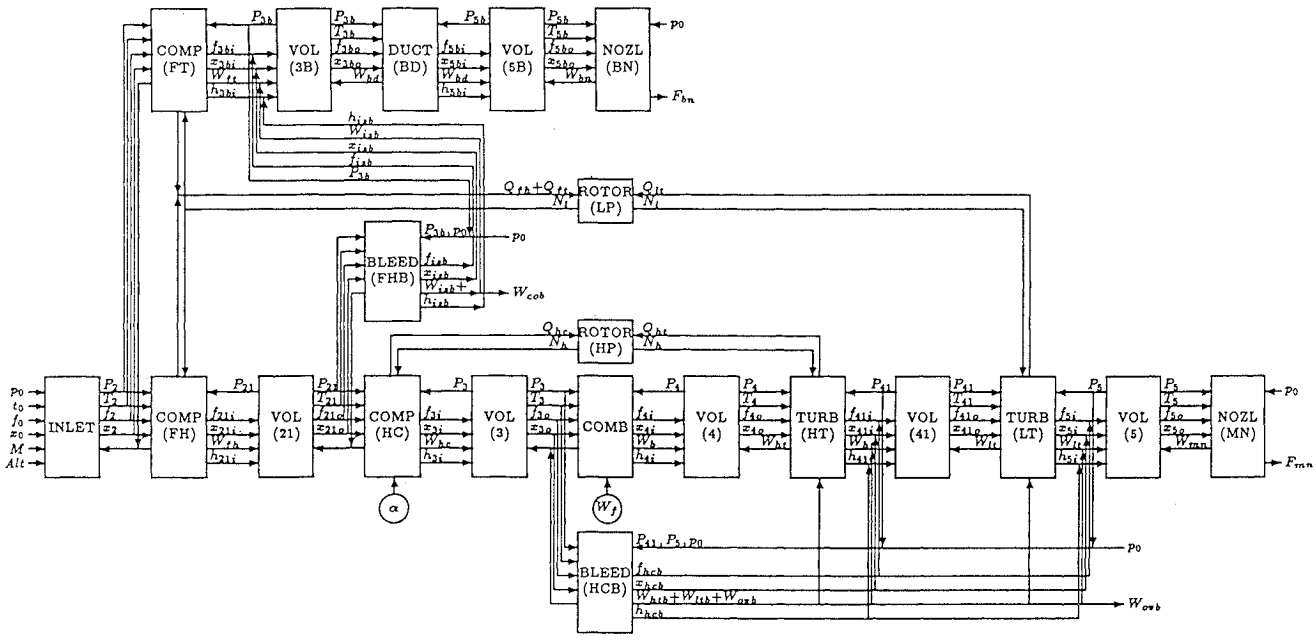

Fig. 2 Simulation block diagram of two-spool turbofan engine.

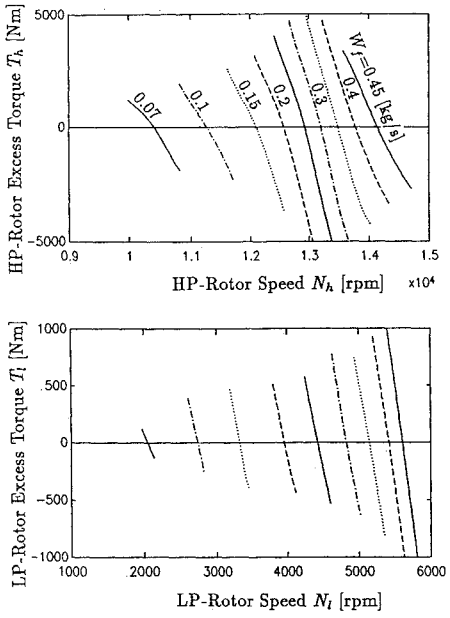

Fig. 3 Excess torque and rotor speed.

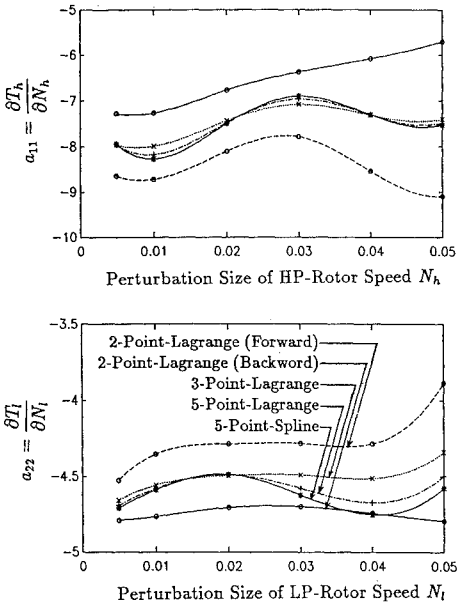

Fig. 4 Effect of perturbation size and formula.

to a rotor speed are considered here. Equation (21) is linearized as in Eq. (3),

$$\delta\dot{N}_h = \frac{\partial T_h}{\partial N_h}\frac{\delta N_h}{I_h} + \frac{\partial T_h}{\partial N_l}\frac{\delta N_l}{I_h} + \cdots = a_{11}\,\delta N_h + a_{12}\delta N_l + \cdots \tag{27}$$

$$\delta\dot{N}_l = \frac{\partial T_l}{\partial N_h}\frac{\delta N_h}{I_l} + \frac{\partial T_l}{\partial N_l}\frac{\delta N_l}{I_l} + \cdots = a_{21}\,\delta N_h + a_{22}\delta N_l + \cdots \tag{28}$$

The excess torque functions of high- and low-pressure rotors, $T_h(N_h)$ and $T_l(N_l)$ are obtained for specified controls W_f and α, as shown in Fig. 3. A cross point of a constant W_f line and zero torque line is a steady operating point. A negative gradient in the neighborhood of the steady point means the system is stable. As seen in Fig. 3, the excess torque function is not a severe nonlinear function in an appropriate region, and therefore, partial derivatives may be obtained by the above-mentioned method. It is important for derivation of system matrices to check whole curves of the RHS of differential equations, $\boldsymbol{f}(\boldsymbol{x}, \boldsymbol{u})$ in Eq. (1). Otherwise, unreasonable results may appear due to local instability, discontinuity, severe nonlinearity, etc. The software developed here includes the capability to display such curves graphically.

Partial derivatives $a_{11} = \partial T_h/\partial N_h$ and $a_{22} = \partial T_l/\partial N_l$ in Eqs. (27) and (28) are slopes of the constant W_f line in Fig. 3. Cross-coupling elements $a_{12} = \partial T_h/\partial N_l = 0$ and $a_{21} = \partial T_l/\partial N_h = 0$ because of the volume dynamics between each component. System matrices A, B, C, D at $W_f = 0.4$ kg/s and $\alpha = 0$ deg are computed for five types of derivation formula, Eqs. (14)–(17), and six perturbation sizes, 0.5, 1, 2, 3, 4, and 5%. Figure 4 shows the effect of the computational formula and perturbation size on the values of A matrix elements a_{11} and a_{22}. Two kinds of two-point Lagrange formulas (forward and backward formulas) generate extreme values of a_{11} and a_{22}, and results by three- and five-point formulas fall between these extremes. The result by a three-point Lagrange is obviously the average of results by a forward and backward two-point Lagrange. If perturbation size is less than 2%, three- and five-point formulas generate close results but still have approximately 10% uncertainty, $-8.6 < a_{11} < -7.6$ and $-4.7 < a_{22} < -4.5$, depending on perturbation size.

B. Corrected System Matrices

In general, the performance of a jet engine is expressed by corrected parameters derived by dimensional analysis. This makes it possible to evaluate engine performance under various atmospheric conditions. If corrected parameters are applied, Eq. (21) can be modified as follows:

$$\frac{\sqrt{\theta}}{\delta}\frac{\dot{N}}{\sqrt{\theta}} = \frac{Q}{\delta\sqrt{\theta}}\frac{\sqrt{\theta}}{N}\frac{1}{I} \tag{29}$$

where corrected rotor speed $N/\sqrt{\theta}$ and corrected power $Q/\delta\sqrt{\theta}$ are used. Then the inverse of the first coefficient in Eq. (29), $\delta/\sqrt{\theta}$, should be the corrected coefficient of time.

At altitude of 11,000 m (36,089 ft) and flight Mach number 0.7, $\delta = 0.310$, and $\theta = 0.831$, and hence $\delta/\sqrt{\theta} = 0.340$. Similarly, at altitude of 3000 m (9,843 ft) and flight Mach number 0.7, $\delta = 0.960$, $\theta = 1.024$, and $\delta/\sqrt{\theta} = 0.948$. This means that the engine response at 11,000 m is 2.79 times slower than that at 3000 m for the same corrected rotor speed and flight Mach number 0.7. A corrected time constant τ and a corrected frequency ω are expressed by $\tau\delta/\sqrt{\theta}$ and $\omega\sqrt{\theta}/\delta$, respectively.

Corrected expressions of A, B, C, and D matrix elements are derived as follows:

$$\begin{aligned}
\tilde{a}_{ij} &= a_{ij}\frac{\sqrt{\theta}}{\delta}\frac{\text{(corrected coefficient of } i\text{th state variable)}}{\text{(corrected coefficient of } j\text{th state variable)}} \\
\tilde{b}_{il} &= b_{il}\frac{\sqrt{\theta}}{\delta}\frac{\text{(corrected coefficient of } i\text{th state variable)}}{\text{(corrected coefficient of } l\text{th control variable)}} \\
\tilde{c}_{kj} &= c_{kj}\frac{\text{(corrected coefficient of } k\text{th output variable)}}{\text{(corrected coefficient of } j\text{th state variable)}} \\
\tilde{d}_{kl} &= d_{kl}\frac{\text{(corrected coefficient of } k\text{th output variable)}}{\text{(corrected coefficient of } l\text{th control variable)}}
\end{aligned} \tag{30}$$

where the tilde denotes a corrected parameter. It should be noted that corrected state, control, and output variables in Eqs. (24)–(26) are $N/\sqrt{\theta}$, m, $u/\delta\sqrt{\theta}$, $W_f/\delta\sqrt{\theta}$, α, P/δ, and T/θ. For example,

$$\begin{aligned}
\tilde{a}_{14} &= a_{14}\frac{\sqrt{\theta}}{\delta}\frac{\text{(corrected coefficient of 1st state variable: } N_h)}{\text{(corrected coefficient of 4th state variable: } u_{21})} \\
&= a_{14}\sqrt{\theta}
\end{aligned} \tag{31}$$

Obviously, corrected diagonal elements of the A matrix are $a_{11}\sqrt{\theta}/\delta, a_{22}\sqrt{\theta}/\delta, \ldots$, with dimension of reciprocal seconds.

Figure 5 shows $a_{11}\sqrt{\theta}/\delta$, $a_{22}\sqrt{\theta}/\delta$, and b_{12}/δ for different operating points at flight Mach numbers 0, 0.4, and 0.8. For example, $a_{11} = -10.818$ and $a_{22} = -3.639$ for $N_l = 4820$ rpm at sea-level

static conditions. At this steady point, a_{11} becomes a minimum and hence the HP rotor's response is the fastest.

The whole corrected elements of system matrices are functions of corrected control variables and flight Mach number:

$$\begin{aligned} \tilde{a}_{ij} &= \tilde{a}_{ij}(W_f/\delta\sqrt{\theta}, \alpha, M), \\ \tilde{b}_{il} &= \tilde{b}_{il}(W_f/\delta\sqrt{\theta}, \alpha, M) \\ \tilde{c}_{kj} &= \tilde{c}_{kj}(W_f/\delta\sqrt{\theta}, \alpha, M), \\ \tilde{d}_{kl} &= \tilde{d}_{kl}(W_f/\delta\sqrt{\theta}, \alpha, M) \end{aligned} \tag{32}$$

The zero elements of system matrices A and B are represented as

$$\begin{pmatrix} \dot{N}_h \\ \dot{N}_l \\ \dot{m}_{21} \\ \dot{u}_{21} \\ \dot{m}_3 \\ \dot{u}_3 \\ \dot{m}_4 \\ \dot{u}_4 \\ \dot{m}_{41} \\ \dot{u}_{41} \\ \dot{m}_5 \\ \dot{u}_5 \\ \dot{m}_{3B} \\ \dot{u}_{3B} \\ \dot{m}_{5B} \\ \dot{u}_{5B} \end{pmatrix} = \begin{pmatrix} \times & 0 & \times & \times & \times & \times & \times & \times & \times & 0 & 0 & 0 & 0 & 0 & 0 \\ 0 & \times & \times & \times & 0 & 0 & 0 & 0 & \times & \times & \times & \times & \times & 0 & 0 \\ \times & \times & \times & \times & \times & \times & 0 & 0 & 0 & 0 & 0 & 0 & \times & \times & 0 & 0 \\ \times & \times & \times & \times & \times & \times & 0 & 0 & 0 & 0 & 0 & 0 & \times & \times & 0 & 0 \\ \times & 0 & \times & \times & \times & \times & \times & \times & 0 & 0 & 0 & 0 & 0 & 0 & 0 & 0 \\ \times & 0 & \times & \times & \times & \times & \times & \times & 0 & 0 & 0 & 0 & 0 & 0 & 0 & 0 \\ 0 & 0 & 0 & 0 & \times & \times & \times & \times & 0 & 0 & 0 & 0 & 0 & 0 & 0 & 0 \\ 0 & 0 & 0 & 0 & \times & \times & \times & \times & 0 & 0 & 0 & 0 & 0 & 0 & 0 & 0 \\ 0 & 0 & 0 & 0 & 0 & 0 & \times & \times & \times & \times & \times & \times & 0 & 0 & 0 & 0 \\ \times & 0 & 0 & 0 & 0 & 0 & \times & \times & \times & \times & \times & \times & 0 & 0 & 0 & 0 \\ 0 & 0 & 0 & 0 & 0 & 0 & 0 & 0 & \times & \times & \times & \times & 0 & 0 & 0 & 0 \\ 0 & \times & 0 & 0 & 0 & 0 & 0 & 0 & \times & \times & \times & \times & 0 & 0 & 0 & 0 \\ 0 & \times & \times & \times & 0 & 0 & 0 & 0 & 0 & 0 & 0 & 0 & \times & \times & \times & \times \\ 0 & \times & \times & \times & 0 & 0 & 0 & 0 & 0 & 0 & 0 & 0 & \times & \times & \times & \times \\ 0 & 0 & 0 & 0 & 0 & 0 & 0 & 0 & 0 & 0 & 0 & 0 & \times & \times & \times & \times \\ 0 & 0 & 0 & 0 & 0 & 0 & 0 & 0 & 0 & 0 & 0 & 0 & \times & \times & \times & \times \end{pmatrix}$$

$$\times \begin{pmatrix} N_h \\ N_l \\ m_{21} \\ u_{21} \\ m_3 \\ u_3 \\ m_4 \\ u_4 \\ m_{41} \\ u_{41} \\ m_5 \\ u_5 \\ m_{3B} \\ u_{3B} \\ m_{5B} \\ u_{5B} \end{pmatrix} + \begin{pmatrix} 0 & \times \\ 0 & 0 \\ 0 & \times \\ 0 & \times \\ 0 & \times \\ 0 & \times \\ \times & 0 \\ \times & 0 \\ 0 & 0 \\ 0 & 0 \\ 0 & 0 \\ 0 & 0 \\ 0 & 0 \\ 0 & 0 \\ 0 & 0 \\ 0 & 0 \end{pmatrix} \begin{pmatrix} W_f \\ \alpha \end{pmatrix} \tag{33}$$

where 0 and × are zero and nonzero elements, respectively. Since state variables of adjacent dynamic modules in Fig. 2 influence each other, the matrix element corresponding to this connection is nonzero. In this turbofan engine case D is a zero matrix.

C. Results

The transfer function is computed using the system matrices as

$$G = C(sI - A)^{-1}B + D \tag{34}$$

Bode diagrams of four transfer function, $g_{11}(s) = N_h/W_f$, $g_{21}(s) = N_l/W_f$, $g_{31}(s) = P_3/W_f$, and $g_{41}(s) = F/W_f$, at N_h of 13,000 and 11,500 rpm using the three-point Lagrange formula with 2% perturbation, are shown in Fig. 6. Actual engine data are also plotted. Good agreement is observed.

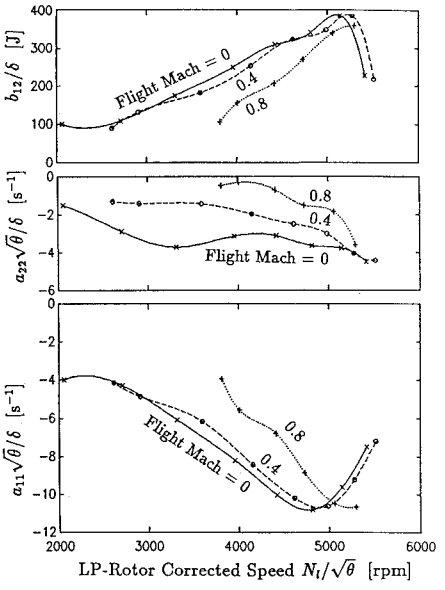

Fig. 5 System matrix elements for different flight condition.

Step responses of linearized models and nonlinear simulation are compared in Fig. 7. Figure 7a shows time responses of LP-rotor speed N_l to step changes of fuel flow W_f. The difference in final values of N_l is due to nonlinearity of the engine. Figure 7b shows time responses normalized by final values. Transient errors of the linearized model to nonlinear simulation are shown in Fig. 7c. The best transient accuracy is obtained by a five-point Lagrange formula with 0.5% perturbation. But other linearized models seem to be reasonable because maximum transient error is around 2%.

VI. Remarks

A. Trimming

Determination of a steady-state equilibrium point, or trimming, is necessary for steady-state analysis of a plant and is performed efficiently by a Newton-Raphson scheme, where the A matrix plays an important role. If the operating point is close to the equilibrium point and A is nonsingular, the equilibrium point is obtained by iteration of Eq. (19). Since this procedure is part of the derivation procedure of the $ABCD$ matrices, inclusion of trimming software is straightforward.

B. Stability of Nonlinear Plant Simulation

Eigenvalues of the A matrix can define a step size of numerical integration for stable nonlinear simulation of a plant. For stable simulation, $h\lambda$ must be in a stable region as defined by the integration method, where h is step size and λ is the eigenvalue of the A matrix. The stable region of Euler's integration, for example, is a disc centered $(-1, 0j)$ with radius 1. If h is defined such that the whole $h\lambda$ are located inside the disc, nonlinear simulation is stable. In the two-spool turbofan engine case, there exists $\lambda \sim (-640, 0j)$ that is farthest from $(-1, 0j)$ and hence the step size should be less than 0.003 s for stable simulation.

C. Limitation

There are some limitations in applying the $ABCD$ matrices derivation procedure developed here:

1) Nonlinear simulation cannot include extreme nonlinearities such as discontinuity, hysteresis, etc. Such elements must be frozen if they exist.

2) Nonlinear simulation must be stable at the steady-state condition. The stability information noted above is helpful for stable simulation.

3) Nonlinear simulation cannot include a time lag, or a difference equation, which is a dynamic element as well as a differential equation. It must be frozen if it exist.

To derive reasonable $ABCD$ matrices, it is recommended to visualize the following items: 1) sensitivity to perturbation size and

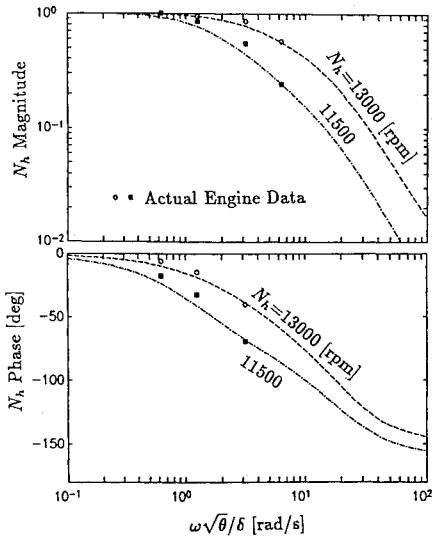

Fig. 6a Frequency response of HP-rotor speed, N_h.

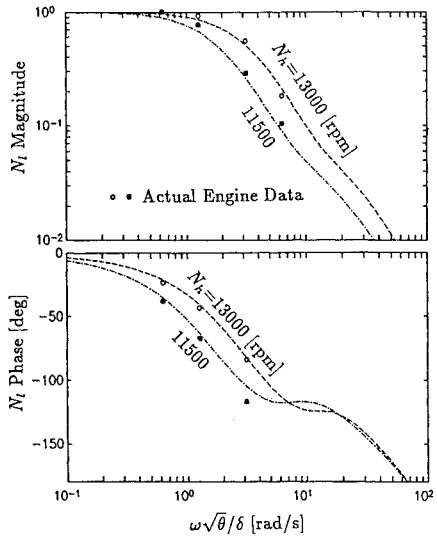

Fig. 6b Frequency response of LP-rotor speed, N_l.

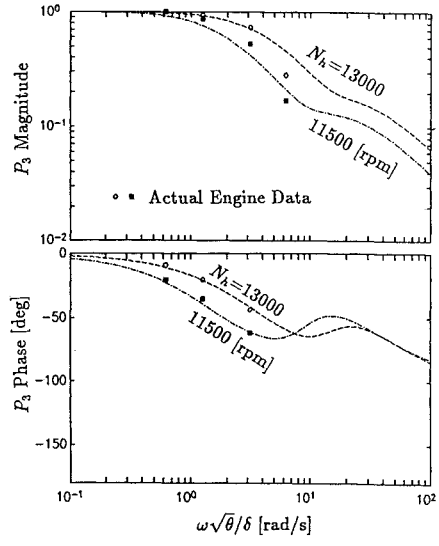

Fig. 6c Frequency response of compressor outlet pressure, P_3.

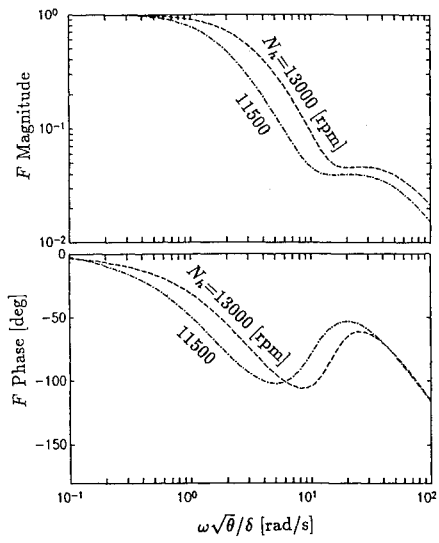

Fig. 6d Frequency response of thrust, F.

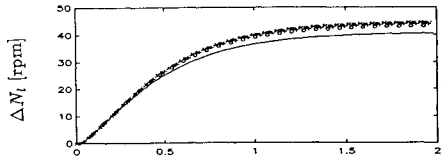

a) Step response

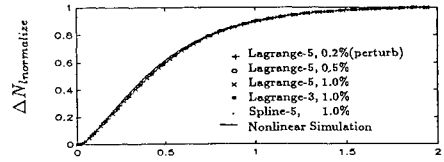

b) Normalized step response

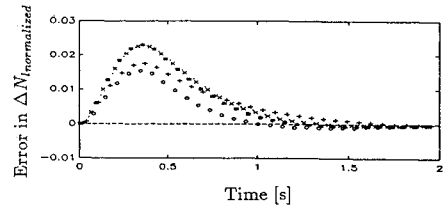

c) Transient error

Fig. 7 Step response of LP-rotor speed to fuel flow change ($M = 0$, $N_h = 13{,}000$ rpm, $W_f = 0.2617$ kg/s, $\Delta W_f = 0.02 W_f$).

formula (see Fig. 4), 2) state derivatives, or the RHS of the differential equation as a function of state (see Fig. 3), and 3) the time history of state derivatives. These visualizations give information on the nonlinearity and stability of nonlinear simulation. The software developed here includes this capability.

VII. Conclusions

A derivation method of a linearized plant model in the form of *ABCD* system matrices is described. The software, combined with nonlinear plant simulation software, perturbs states and controls around an operating point to determine the elements of *ABCD* matrices. To illustrate the capability of the software developed, system matrices of a two-spool turbofan engine are obtained and compared with actual engine data. Sensitivity to perturbation size and formula, linearity of state derivatives, uncertainty due to modeling are discussed. In this example, the best results are obtained by a five-point Lagrange formula with 0.5% perturbation, but a three-point formula that is computationally efficient still brings reasonable results. Corrected expressions of system matrices are introduced to extend the data base to the whole flight envelope.

Acknowledgments

This work was supported in part by the Hyper/Supersonic Transport Propulsion System program of AIST, MITI. The author thanks M. Morita and R. Yanagi of the National Aerospace Laboratory for their support in the preparation of actual engine data and S. Matsui of Kyokuto Boeki Kaisha for his support in programming.

References

[1]DeHoff, R. L., Hall, W. E., Jr., and Adams, R. J., "F100 Multivariable Control Synthesis Program," Air Force Aero-Propulsion Laboratory, AFAPL-TR-77-35, Ohio, Jun. 1977.

[2]Geyser, L. C., "DYGABCD—A Program for Calculating Linear A, B, C, and D Matrices from a Nonlinear Dynamic Engine Simulation," NASA TP 1295, Sept. 1978.

[3]Miller, R. J., and Hackney, R. D., "F100 Multivariable Control System Engine Models/Design Criteria," Air Force Aero-Propulsion Laboratory, AFAPL-TR-76-74, Ohio, Nov. 1976.

[4]Ljung, L., *System Identification*, Prentice-Hall, New York, 1987.

[5]*SIMULAB User's Guide*, MathWorks, Natick, MA, 1991.

[6]*EASY5 User's Guide*, Boeing Computer Services, Seattle, WA, 1984.

[7]*AD100 Hardware Reference Manual* and *ADSIM Reference Manual*, Applied Dynamics International, Ann Arbor, MI, 1988.

[8]Sugiyama, N., "Generalized High Speed Simulation of Gas Turbine Engines," American Society of Mechanical Engineers, ASME Paper 90-GT-270, New York, June 1990.